Field-emission spectrum of a nanometer-size supported gold cluster: Theory and experiment

M. E. Lin and R. Reifenberger
Department of Physics, Purdue University, West Lafayette, Indiana 47907

R. P. Andres
School of Chemical Engineering, Purdue University, West Lafayette, Indiana 47907
(Received 24 January 1992; revised manuscript received 27 July 1992)

The electron-energy spectrum of a single 1-nm-diam Au cluster supported on a W substrate has been studied by measuring the distribution of electrons field emitted from the cluster. A resonance-tunneling theory is described that reproduces the salient features of the experimental spectrum and relates it to the electronic structure of the supported cluster.

I. INTRODUCTION

It is now well established that the physical and chemical properties of small clusters with diameters between ~ 1 and ~ 10 nm can be entirely different from those of the bulk.[1] Small metal clusters, for example, exhibit a size-dependent electronic structure. In order to improve our understanding of this behavior, it is important to develop experimental techniques capable of resolving the electronic structure of nanometer-size metal clusters. In the case of free-space clusters, cluster beam measurements can provide this information. In the case of both alkali[2,3] and transition metals,[4] the mass spectra of ionized free-space clusters show peaks at certain "magic" mass numbers providing evidence for a shell-like organization of electron states. Photoionization studies of unsupported potassium clusters also exhibit evidence of this shell structure,[5] as do photoelectron studies of copper anion clusters.[6]

However, when a cluster is adsorbed onto a substrate, the survival (and modification) of the cluster's electronic states becomes an important issue that has yet to be satisfactorily addressed. This is a question of considerable interest, since supported metal clusters are important in a wide variety of electronic and chemical applications. Samples of metal clusters deposited on flat substrates in ultrahigh vacuum (UHV) have been studied by photoelectron spectroscopy.[7–9] These studies show a narrowing of the valence band and a decrease in the core-electron binding energies as cluster size decreases. Unfortunately, this technique does not have the sensitivity to explore the properties of an individual cluster and the experimental measurement is always a convolution over a large number of clusters. Thus, there is the possibility that clusters of different size and configuration contribute to the spectra. In a previous paper,[10] we described a way to overcome this difficulty by measuring the energy distribution of electrons field emitted from individual nanometer-size clusters supported on a conducting substrate. These data revealed important information on the electronic structure of supported metal clusters. In this paper we provide the details of the resonance-tunneling theory used to interpret the field-emission spectra from a supported cluster.

The remainder of this paper is organized in the following way. In Sec. II we briefly review the underlying principles of field emission. Section III extends these results and presents a resonance-tunneling theory of weakly adsorbed metal clusters under the influence of an applied electric field. Section IV presents data which show how the discrete cluster electronic states of a 1-nm-diam Au cluster can be probed using field-emission techniques. The theory developed in Sec. III is used to interpret the structure observed for this 1-nm-diam cluster. In Sec. V the important conclusions obtained from this study are summarized.

II. FIELD-EMISSION THEORY

The theory of field emission is concerned with the calculation of $j(E)$, the number of electrons of mass m emitted per unit area per unit time with energy between E and $E+dE$, while an electric field F is applied in the z direction.[11] The details of this calculation are well described in the literature and only the important results will be presented here. This calculation requires an integration over all possible wave vectors $\mathbf{k}=(k_z,k_\parallel)$,

$$j(E)dE=\int_E^{E+dE} N(\mathbf{k})|T(k_z,E)|^2\frac{d^3k}{(2\pi)^3}\,, \qquad (1)$$

where $N(\mathbf{k})$ is the number of electrons with wave vector $\mathbf{k}$ incident on the barrier per unit time per unit area and $|T(k_z,E)|^2$ is the transmission probability through the surface potential barrier. The appropriate barrier is usually a metal with a Fermi level E_F and work function ϕ. The metal-vacuum interface is described in one dimension by an image-rounded barrier given by

$$V(z)=\begin{cases} E_F+\phi-\dfrac{e^2}{4z}-eFz & \text{for } z>z_c \\ 0 & \text{for } z<z_c\,, \end{cases} \qquad (2)$$

where z_c is determined by $V(z_c)=0$. Using the WKB approximation to estimate $T(k_z,E)$ and a free-electron ap-

proximation to evaluate $N(\mathbf{k})$, the standard result for the distribution of emitted electrons is obtained,

$$j_0(E)=\frac{md_E f(E)}{2\pi^2\hbar^3} \times\exp\left[\frac{-4}{3}\left[\frac{2m}{\hbar^2}\right]^{1/2}\frac{(\phi+E_F-E)^{3/2}}{eF}v(y)\right], \quad (3)$$

where

$$\frac{1}{d_E}=2\left[\frac{2m}{\hbar^2}\right]^{1/2}\frac{(\phi+E_F-E)^{1/2}}{eF}t(y), \quad (4)$$

$v(y),t(y)$ are slowly varying, tabulated[12] functions of $y=(e^3F)^{1/2}/(\phi)$ and $f(E)$ is the Fermi-Dirac function. The shape and location of the field-emission energy distribution is shown schematically in Fig. 1(a). The shape of $j_0(E)$ is roughly governed by the temperature of the emitter for $E>E_F$ and the transmission probability through the metal-vacuum interface for $E<E_F$. An experimental measurement of this energy distribution involves further convolution of Eq. (3) with a symmetric Gaussian window function that accounts for the finite-energy resolution of the energy analyzer. It is an experimental fact that Eq. (3) describes well the overall shape of the distribution of electrons emitted from field-emission tips fabricated from a variety of refractory metals.[11]

Equation (3) can be further integrated to give the total electrical current

$$J(F)=e\int_{-\infty}^{\infty}j_0(E)dE = A'F^2e^{-(B'\phi^{3/2}/F)}, \quad (5)$$

where A' and B' are known constants.[13] This result, known as the Fowler-Nordheim (FN) equation, predicts a plot of $\ln[j(F)/F^2]$ vs $1/F$ will give a straight line with a slope related to the work function ϕ of the emitting surface. Use of this equation has provided much of the systematic information now available on the work function of the various crystal faces of pure metals.

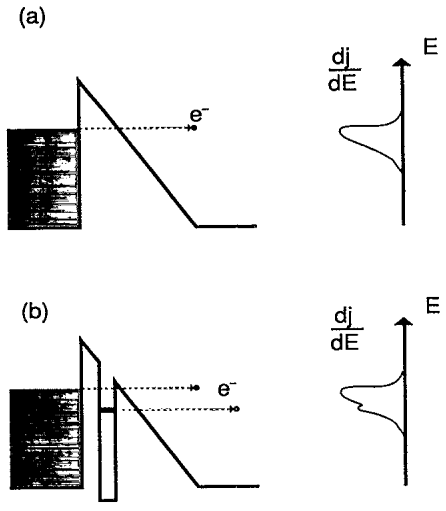

FIG. 1. (a) The standard triangular field-emission potential barrier showing the location in energy of a typical field-emission energy distribution from a metal tip. (b) The field-emission potential barrier modified by the adsorption of an atom. Resonance tunneling can produce an electron-emission spectrum that mirrors the highest occupied states of the adsorbed atom.

In the following section we will apply these basic ideas of field emission to learn more about the electronic states of a supported metal cluster. The major modification that is required is to replace the free-electron supply function $N(\mathbf{k})$ in Eq. (1) with the quantized density of states for a nanometer-size cluster absorbed at a metal-vacuum interface.

III. ELECTRON EMISSION FROM A SUPPORTED CLUSTER

In this section a resonance-tunneling theory of electron emission from a nanometer-size cluster in the presence of a strong electric field when the cluster is weakly coupled to a conducting substrate is described. When a cluster is brought from infinity up to a metal surface, two important issues must be addressed. The first concerns whether the quantized electron states of the cluster are destroyed upon deposition. The second is how the substrate modifies the electron states of the cluster. Field-emission experiments can answer both questions, but introduce a further complication, i.e., the influence of the applied electric field. For a gold cluster with a diameter less than ~ 1.2 nm, it can be estimated that the applied field penetrates a shell consisting of $\sim 50\%$ of the cluster volume. In this case, the applied field becomes an important perturbation on the cluster states and influences the energy distribution of the field-emitted electrons.

In the remainder of this section a model, based on a resonance-tunneling theory developed for a single atom adsorbed on a field-emission tip by Gadzuk,[14] is presented. The utility of the model is that it allows an estimate of the tunneling enhancement factor and the energy shifts for a supported metal cluster in an applied electric field.

A. Resonance tunneling from an individual-supported cluster

Duke and Alferieff[15] have emphasized the importance of resonance-tunneling effects on field emission through atoms adsorbed on an emitter. It is generally recognized that emission from the discrete atomic levels is shifted, broadened, and enhanced by interaction with the substrate. A schematic illustration of field emission through an atom supported on a metal substrate is shown in Fig. 1(b) where the additional feature in the energy spectrum is due to electron emission from an atomic state. This additional emission is often characterized by a current enhancement factor $R(E)$, defined experimentally by the ratio

$$R(E)\equiv\frac{dj}{dE}\Big/\frac{dj_0}{dE}, \quad (6)$$

where dj_0/dE is the energy distribution without the atom and dj/dE is the distribution with the adsorbed atom. Similar enhancements can be anticipated when studying electron emission from supported nanometer-size clusters.

Following Gadzuk,[14] a resonance-tunneling approach is used to discuss how electrons will tunnel from a cluster. In this approach the full Hamiltonian of the system is divided into three parts, the first and second representing the unperturbed Hamiltonians of the substrate and vacuum as if the cluster were not present. The third part is the operator which connects the two sides and determines the enhanced rate of tunneling.

In the absence of the cluster [see Fig. 1(a)], the Hamiltonian for field emission can be written as

$$H=E_K+U_m+U_F=H_0^m+U_F=H_0^F+U_m \ , \tag{7}$$

where E_K is the kinetic-energy operator, U_m, the potential of the metal substrate, is given by

$$U_m=\begin{cases}0 & \text{if } z<0\\ E_F+\phi_m & \text{if } z\geq 0 \ ,\end{cases} \tag{8}$$

and U_F, the potential of the applied field, is equal to $-eFz$ for $z\geq 0$. Using the Oppenheimer scheme developed to discuss the field ionization of an isolated hydrogen atom,[16] the tunneling matrix can be written as

$$T_0=\langle f|U_F|m\rangle \ , \tag{9}$$

where $|f\rangle$ and $|m\rangle$ are the eigenstates of the Hamiltonians H_0^F and H_0^m, respectively.

When a cluster is deposited on the field-emission tip, a third part must be added to the Hamiltonian given by Eq. (7). The new Hamiltonian, which includes information about the cluster and field penetration into the cluster, can be written

$$H=E_K+U_m+(U_c+U_F')+U_F \ , \tag{10}$$

where U_c is the potential of the free-space cluster. U_F', which accounts for the shielding effect of the cluster on the applied field, is expressed as

$$U_F'=\begin{cases}0, & z<0\\ +eFz, & 0<z<d\\ +eFz+eV_{\rm fp}, & d<z<d+2R\\ +eF(d+2R), & z>d+2R \ .\end{cases} \tag{11}$$

In Eq. (11), d is the distance between the surface of the metal substrate and the surface of the cluster, R is the radius of the cluster [see Fig. 2(a)], and $V_{\rm fp}$ is a term to be calculated later that measures the extent of field penetration into the cluster.

For clusters, Gadzuk's definition[11] of an atomic state $|a_0\rangle$ must be replaced with the appropriate cluster state $|c_0\rangle$. The energy shift of a discrete cluster state ($|c_0\rangle$) then becomes

$$\Delta E=\langle c_0|U_m+U_F'|c_0\rangle \ . \tag{12}$$

There are a few approximations in this model that should be mentioned. First, the work function and the Fermi level of the cluster have been taken to be equal to that of the metal substrate. If there is a difference between the work function of the cluster and that of the substrate, then U_F' should be modified by simply adding the difference between the two work functions. Second, only the lowest-order perturbation has been considered. For small clusters weakly coupled to the substrate, it seems reasonable to approximate the energy shift using the field-modified potential given by U_F'. Other interactions are neglected.

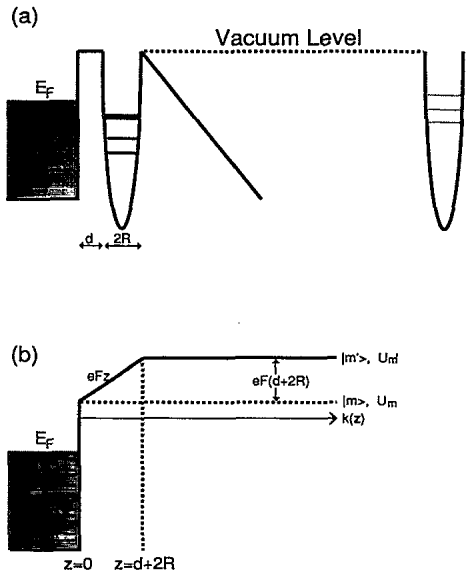

FIG. 2. (a) The change in energy states as a free-space cluster is deposited onto a metal substrate. The discrete energy states are shifted down and broadened by the applied field and by interaction with the substrate. The potential barrier between substrate and cluster is assumed to be flat in order to simplify the calculations. (b) The modified substrate potential (U_m'). The horizontal dotted line represents the potential U_m. The wave vector $k(z)$ of the tunneling electron is also shown.

If the wave function of each cluster state is localized inside the cluster and an infinite harmonic well is assumed to adequately describe the free-space cluster,[2] Eq. (12) can be further simplified. The only contribution to the energy shift comes from the region $d<z<d+2R$. In this region, the term containing the applied field ($\langle c_0|eFz|c_0\rangle$) can be readily evaluated as

$$\langle c_0|eFz|c_0\rangle \propto \int_0^R\int_0^{\pi}\int_0^{2\pi} f(r)Y_{lm}^*\cos(\theta)\sin(\theta) \times Y_{lm}\,d\phi\,d\theta\,dr=0 \ . \tag{13}$$

Using this result, the energy shift simplifies to

$$\Delta E\approx\langle c_0|eV_{\rm fp}|c_0\rangle \ . \tag{14}$$

Thus, the only nonzero, first-order perturbation to the energy levels of the cluster is caused by field penetration.

To facilitate an estimate of lifetime broadening and resonance effects, a new modified substrate potential U_m' is defined as

$$U_m'=\begin{cases}0, & z<0\\ U_m+eFz, & 0<z<d+2R\\ U_m+eF(d+2R), & z>d+2R\end{cases} \tag{15}$$

[see Fig. 2(b)]. Note that using this definition for U'_m, we have $U'_m + eV_{fp} = U_m + U'_F$. Following Gadzuk,[11] the tunneling matrix element can be written as

$$T \approx \langle f|U_F|m'\rangle + \frac{\langle f|U_F|c\rangle\langle c|U_F|m'\rangle}{E - E_{c'} - i\Gamma} . \quad (16)$$

Within the Oppenheimer scheme, the emission current is proportional to $|T|^2$. Thus, from Eq. (6), the resonance-enhancement factor, $R(E) = |T|^2/|T_0|^2$, will be given by

$$R(E) \approx |B|^2 \left[1 + \frac{T_c^2(E)}{(E - E_{c'})^2 + \Gamma^2} + \frac{2(E - E_{c'})|T_c(E)|}{(E - E_{c'})^2 + \Gamma^2} \right] , \quad (17)$$

where

$$B = \frac{\langle f|U_F|m'\rangle}{\langle f|U_F|m\rangle} \quad (18)$$

and

$$T_c(E) = \frac{\langle f|U_F|c\rangle\langle c|U_F|m\rangle}{\langle f|U_F|m\rangle} . \quad (19)$$

The term $|B|^2$ acts as a scaling factor between the metal potential and the field-modified model potential. Without the field or cluster, the value of $R(E)$ should be unity, which is the first term in the parentheses of Eq. (17). The second term in the parentheses represents resonance-tunneling effects. The last term represents the interaction between direct tunneling and resonance tunneling. These matrix elements can be further evaluated by WKB methods as discussed below.

B. Field penetration into a supported Au cluster

As discussed above, supported clusters will be affected by both the substrate and the applied field. In what follows, we assume the 6*s* electrons of the gold atoms in the cluster to be decoupled and free to move under the influence of the infinite harmonic-well potential specified by

$$U_c(r) = -U_0 + \tfrac{1}{2} m\omega^2 r^2 , \quad (20)$$

where U_0 is the sum of the Fermi energy and work function of Au. The energy spectrum of these electrons is discrete and the eigenstates are defined by[17]

$$|c_0\rangle = A_{nlm} r^l e^{(-\lambda r^2/2)} {}_1F_1(-n; l + \tfrac{3}{2}; \lambda r^2) Y_{l,m}(\theta,\phi) , \quad (21)$$

where $\lambda = m\omega/\hbar$, and ${}_1F_1$ is a hypergeometric series that is a function of the principal quantum number n and the angular momentum l. Here, the Hamiltonian is defined as

$$H = E_K + U'_m + U_c + U_F + eV_{fp} . \quad (22)$$

If the potential barrier in the region $0 < z < d$ is flat as drawn in Fig. 2(a), the energy shift is given by

$$\Delta E \simeq \langle c_0|eV_{fp}|c_0\rangle + \phi_{s-c} , \quad (23)$$

where ϕ_{s-c} is the work-function difference between the substrate and the Au cluster. This quantity can be estimated by (i) measuring the work function of the W substrate using standard Fowler-Nordheim techniques[11] and (ii) relying on estimates of the size-dependent work function of supported Au clusters determined by Castro *et al.*[18] The induced potential due to field penetration was discussed previously[10] and is given by

$$V_{fp} \approx \frac{-C\lambda_D^2}{r^2} \left[\frac{2r}{\lambda_D} \cosh(r/\lambda_D) - 2\sinh(r/\lambda_D) \right] , \quad (24)$$

where λ_D, the Debye wavelength, determines the penetration of the electric field into the cluster.

IV. RESULTS FOR A 1-nm-diam Au CLUSTER

In this section we discuss in more detail the structure obtained in the energy spectrum obtained from a 1-nm-diam Au cluster supported on W(110).[10] We demonstrate using the analysis scheme discussed above that the observed spectrum can be related to the discrete energy levels of the free cluster. The experimental energy distribution, which was published previously, is shown in Fig. 3. The data are plotted as electron flux versus electron energy, with the zero of energy defined as the Fermi level (E_F) of the substrate. In this experiment, E_F was accurately determined by thermally desorbing the cluster from the tip and measuring the energy distribution from the underlying W tip.[10] The energy distribution from the substrate was analyzed by the established theory of field emission outlined in Sec. II. Both E_F and the work function of the substrate were obtained in this way. These data clearly show that the cluster states are shifted ~ 2.5 eV below E_F of the substrate and indicate that the electronic states of a 1-nm-diam Au cluster need not be pinned to the substrate's Fermi level.

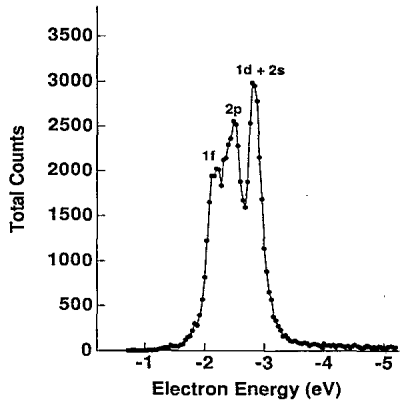

FIG. 3. The field-emission spectrum observed with an applied voltage of 2550 V from a Au cluster of ~1-nm diam. The electron-energy distribution is dominated by three prominent peaks that are related to the electronic structure of the gold cluster. The labels identify the origin of the peaks based on the electron-shell model calculation discussed in the text. Reproduced from Ref. 10.

A number of distinct features or peaks, which mirror the quantized electron states of the supported cluster, are evident in Fig. 3. A characteristic of the measured electron-energy distribution is the sensitivity of the individual peak heights to the applied electric field, indicating resonant enhancement of the tunneling current. The applied field also controls the position in energy of the observed peaks. By contrast, the electrons emitted from the substrate show no shift with field. Careful study also reveals no emission from states at energies near the E_F of the substrate when the cluster is present, even though counting intervals extending up to a 5-min dwell time per channel were employed.

A. Estimate of energy shifts

It remains to identify the electronic states responsible for the observed structure in the field-emission spectrum. From Sec. III, the modified theory of resonance tunneling can be employed and the expected cluster states can be calculated from Eqs. (23) and (24). For a 40-atom cluster (diameter ≈ 1.08 nm), the filled electronic shells are $1s$, $1p$, $2s$, $1d$, $1f$, and $2p$ for an infinite harmonic-well potential. In the field-emission energy spectrum, only the highest two degenerate states ($2s, 1d$ and $1f, 2p$) are observable due to the rapid fall-off of the transmission probabilities for the other states. The wave functions of these four shells are, respectively,

$$\psi_{100}=c_s e^{-\lambda r^2/2}(1-2\lambda r^2/3)Y_{00} , \tag{25}$$

$$\psi_{02m}=c_d e^{-\lambda r^2/2} r^2 Y_{2m} , \tag{26}$$

$$\psi_{03m}=c_f e^{-\lambda r^2/2} r^3 Y_{3m} , \tag{27}$$

$$\psi_{11m}=c_p e^{-\lambda r^2/2}(1-2\lambda r^2/5) r Y_{1m} , \tag{28}$$

where λ is the radial decay constant of the wave function. The normalization constants are equal to

$$\begin{aligned} c_s &= \left[\frac{6\lambda^{3/2}}{\pi^{1/2}}\right]^{1/2} , \\ c_d &= \left[\frac{16\lambda^{7/2}}{15\pi^{1/2}}\right]^{1/2} , \\ c_f &= \left[\frac{32\lambda^{9/2}}{105\pi^{1/2}}\right]^{1/2} , \\ c_p &= \left[\frac{10\lambda^{5/2}}{3\pi^{1/2}}\right]^{1/2} . \end{aligned} \tag{29}$$

Equations (23) and (24) can be used to estimate the field-dependent energy shift for the various shell states (n,l) of the cluster. For example, if ψ_{100} is considered,

$$\Delta E_{100}=-C\lambda_D^2\left[\frac{6\lambda^{3/2}}{\pi^{1/2}}\right]\int_0^R e^{-\lambda r^2}(1-2\lambda r^2/3)^2 \times\left[\frac{2r}{\lambda_D}\cosh(r/\lambda_D)\right]dr . \tag{30}$$

In order to simplify the integration, the upper limit of R is set to infinity rather than the radius of the cluster. For a 1-nm-diam cluster, the error is less than 5% if this approximation is made. Thus, Eq. (30) can be rewritten as

$$\Delta E_{100}=K_s(I_1/\lambda_D-4\lambda I_3/3\lambda_D+4\lambda^2 I_5/9\lambda_D-I_0 +4\lambda I_2/3-4\lambda^2 I_4/9) , \tag{31}$$

where

$$K_s=-C\lambda_D^2 c_s^2 , \tag{32}$$

and

$$I_{2n+1}=\frac{2}{\lambda_D}\int_0^\infty e^{-\lambda r^2} r^{2n+1}\cosh(r/\lambda_D)dr , \tag{33}$$

$$I_{2n}=2\int_0^\infty e^{-\lambda r^2} r^{2n}\sinh(r/\lambda_D)dr , \tag{34}$$

with $n=0,1,2,\ldots$. The shift in energy of the other states can likewise be written as

$$\Delta E_{02m}=K_d(I_5/\lambda_D-I_4) , \tag{35}$$

$$\Delta E_{03m}=K_f(I_7/\lambda_D-I_6) , \tag{36}$$

and

$$\Delta E_{11m}=K_p(I_3/\lambda_D-4\lambda I_5/5\lambda_D+4\lambda^2 I_7/25\lambda_D -I_2+4\lambda I_4/5-4\lambda^2 I_6/25) . \tag{37}$$

The functions I_{2n+1} and I_{2n} can be evaluated as follows:

$$I_{2n+1}=\Gamma(2n+2)(2\lambda)^{2n} e^{1/(8\lambda\lambda_D^2)} \times[D_{-2n-2}(-\chi)+D_{-2n-2}(\chi)], \tag{38}$$

$$I_{2n}=\Gamma(2n+1)(2\lambda)^{-(2n+1)/2} e^{1/(8\lambda\lambda_D^2)} \times[D_{-2n-1}(-\chi)-D_{-2n-1}(\chi)] , \tag{39}$$

where $\chi=(2\lambda)^{-1/2}/\lambda_D$ and $D_{-n}(\chi)$ is the parabolic cylinder function.[19] A general conclusion reached from this analysis is that the cluster states shift to lower energies as the applied electric field increases.

The two parameters, λ_D and λ, control the penetration of the electric field into the cluster and the radial decay of the wave function, respectively. These parameters can be iteratively adjusted until the energy shifts of the various shell states are in agreement with the observed peak positions in the emission spectra for a given external electric field such as the data for an applied voltage of 2550 V shown in Fig. 3. The results of this procedure were presented in Fig. 4 of Ref. 10. Reasonable agreement between the position of the peaks predicted theoretically and measured experimentally are found. This allows a tentative identification of the electronic states responsible for the structure observed (see labels in Fig. 3).

B. Lifetime-broadening and resonance-tunneling effects

In addition to an energy shift, a lifetime-broadening and a resonance-tunneling factor is also required to fully explain each peak. These factors control the width of the peaks as well as the relative height of the peaks observed.

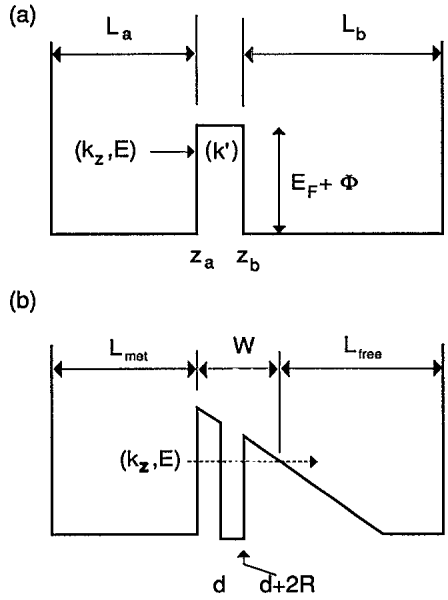

FIG. 4. (a) The parameters required to estimate the tunneling matrix element through a simple square-well potential. (b) The same parameters for the potential barrier of interest.

Although it is difficult to obtain quantitative values for the resonance tunneling factors [see Eq. (17)], it is worthwhile to estimate these factors in order to check the consistency of our theoretical model. First, we estimate the resonance-tunneling factor B using Eq. (17). The energy dependence in B is roughly proportional to

$$B \propto e^{-(k_z'+k_z)z}\big|_{z=d} , \tag{40}$$

where

$$k_z'=\sqrt{2m/\hbar^2}\left[\frac{(E_F+\phi-E)^{1/2}}{2}+\frac{(E_F+\phi-E+eFR)^{1/2}}{2}\right] , \tag{41}$$

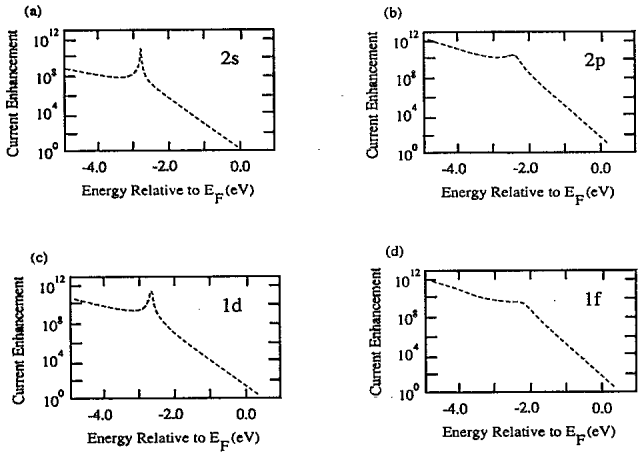

FIG. 5. The resonance-tunneling enhancement factors for the energy levels of the infinite oscillator well model for a nominal 1-nm cluster. (a) 2s, (b) 2p, (c) 1d, (d) 1f.

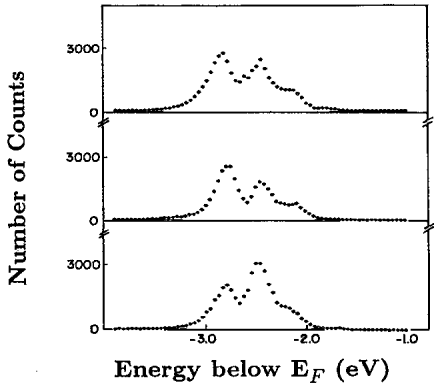

FIG. 6. Evidence for variation in resonance-tunneling effects for a 1-nm-diam cluster can be obtained by measuring the field-emission energy distribution as a function of time. For the data shown, the applied electric field is the same. In (a), the energy distribution measured initially, (b) 2 h later, and (c) 4 h later.

$$k_z=\sqrt{2m/\hbar^2}[(E_F+\phi-E)^{1/2}] , \tag{42}$$

and R is the radius of the cluster.

Next, the other factors in Eq. (17) can be conveniently estimated using Harrison's WKB method.[20] This method estimates the tunneling matrix element for an electron through a barrier with classical turning points described by z_a and z_b [see Fig. 4(a)] by

$$M_{ab}=\frac{\hbar^2}{2m}\sqrt{k_z/L_a}\sqrt{k_z/L_b}\,e^{-k'(z_a-z_b)} , \tag{43}$$

where L_a and L_b measure the extent of the classically accessible region on either side of the barrier. The average wave vector k' of the electron inside the tunnel barrier is given, for the case considered here, by

$$k'=\tfrac{1}{2}[(2m/\hbar^2)(E_F+\phi-E)]^{1/2} . \tag{44}$$

The factors needed to evaluate T_c [Eq. (19)] can be approximated using the same approach [see Fig. 4(b)]:

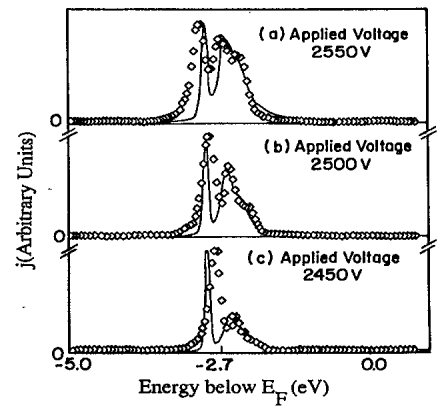

FIG. 7. The theoretical fit to the field-emission energy distribution from ~1-nm-diam cluster as a function of the applied electric field. The approximate value of the electric field F is related to the applied voltage V by $F=\beta V$, where $\beta\sim3.2\times10^4$ cm^{-1} for the cluster studied here. The lifetime-broadening constants used in this fit are given in Table I.

TABLE I. The lifetime-broadening constants required for different applied voltages. The approximate value of the electric field F is related to the applied voltage V by $F=\beta V$, where $\beta \sim 3.2\times 10^4$ cm^{-1} for the cluster studied here.

Cluster state	Peak position	2450 V	2500 V	2550 V
$1f$	−2.2 eV	0.19	0.19	0.19
$2p$	−2.5 eV	0.09	0.08	0.11
$1d$	−2.8 eV	0.002	0.01	0.019
$2s$	−2.8 eV	0.003	0.003	0.003

$$\langle f|V_F|c\rangle \simeq \frac{\hbar^2}{2m}\sqrt{K_z/2R}\,|_{z=R}\sqrt{K_z/L_{\text{free}}}|_{z=W-d-2R}\,e^{-K_z(W-d-2Rr)}, \tag{45}$$

$$\langle c|V_F|m\rangle \simeq \frac{\hbar^2}{2m}\sqrt{K_z/2R}\,|_{z=-R}\sqrt{K_z/L_{\text{met}}}|_{z=-d-R}\,e^{-K_z d}, \tag{46}$$

$$\langle f|V_F|m\rangle \simeq \frac{\hbar^2}{2m}\sqrt{K_z/L_{\text{met}}}|_{z=-d-R}\sqrt{K_z/L_{\text{free}}}|_{z=W-d-2R}\,e^{-K_z W}. \tag{47}$$

Thus, from Eq. (19), the tunneling matrix T_c is

$$T_c \simeq \frac{\hbar^2}{2m}\sqrt{K_z/2R}\,|_{z=R}\sqrt{K_z/2R}\,|_{z=-R}\,e^{2K_z R}. \tag{48}$$

The resonance-tunneling enhancement for each cluster state can now be estimated and the results are plotted in Fig. 5.

The lifetime-broadening constant Γ is more difficult to estimate because a knowledge of the shape of the potential barrier between the cluster and substrate as well as the electronic wave functions outside the cluster boundary are required. In addition, experimental evidence indicates that the resonance-tunneling factors vary with time (see Fig. 6). From these data, one notices that, while peak positions are essentially constant for a given external electric field, the relative heights of the peaks change considerably. This indicates that the coupling between the cluster and the substrate is not constant. We therefore treat the lifetime-broadening constants as a set of adjustable parameters.

After approximating the current enhancement as described above, a set of lifetime-broadening constants in Eq. (17) was chosen to fit the data. Figure 7 shows the resulting comparison between the data and theory. The lifetime-broadening constants, required to give reasonable fits to the data, are tabulated in Table I. These results show a trend which indicates that the highest occupied states are broadened the most, while the states more tightly bound exhibit little broadening. Furthermore, while the $1f$, $2p$, and $2s$ levels do not exhibit strong field-dependent lifetime broadening, the $1d$ state seems very sensitive to the applied field.

V. SUMMARY AND CONCLUSIONS

Experiments that measure the energy spectrum of electrons field emitted from Au clusters supported on a tungsten substrate have been performed. The data show that the quantum states of a nanometer-size cluster can survive after deposition and need not be pinned to the Fermi level of the substrate. The emission spectrum observed for a Au cluster with a diameter of ~ 1 nm was compared to predictions of a resonance-tunneling model that assumes a shell model for the quantum electron levels of the cluster and reasonable agreement was obtained.

Although field emission from a single cluster provides important information about the cluster's electronic properties, the measurements are not yet refined enough to provide a detailed understanding of electronic structure as a function of cluster size. The reason a more quantitative understanding is not yet possible is twofold. First, it is difficult to determine experimentally the precise size and atomic configuration of the cluster under study. Second, the coupling of the cluster states to those of the underlying substrate cannot yet be controlled experimentally.

In spite of these shortcomings, valuable information about the electronic properties of individual, supported metal clusters can be obtained. For an ~ 1-nm-diam gold cluster, quantitative information can be extracted from the field-emission spectrum that allows identification of the energy levels.

ACKNOWLEDGMENT

This work was partially supported by the U.S. Department of Energy under Grant No. DE-FG02-88ER45162.

[1] R. P. Andres, R. S. Averback, W. L. Brown, L. E. Brus, W. A. Goddard, A. Kaldor, S. G. Louie, M. Moscovits, P. S. Peercy, S. J. Riley, R. W. Siegel, F. Spaepen, and Y. Wang, J. Mater. Res. **4**, 704 (1989).

[2] W. D. Knight, K. Clemenger, W. A. de Heer, W. A. Saunders, M. Y. Chou, and M. L. Cohen, Phys. Rev. Lett. **52**, 2141 (1984).

[3] S. Bjørnholm, J. Borggreen, O. Echt, K. Hansen, J. Pedersen, and H. D. Rasmussen, Phys. Rev. Lett. **65**, 1627 (1990).

[4] I. Katakuse, T. Ichihara, Y. Fujita, T. Matsuo, T. Sakurai, and

H. Tsuda, Int. J. Mass. Spectrom. Ion Phys. **67**, 229 (1985).
[5]W. A. Saunders, K. Clemenger, W. A. deHeer, and W. D. Knight, Phys. Rev. B **32**, 1366 (1985).
[6]C. L. Pettiette, S. H. Yang, M. J. Craycraft, J. Conceicao, R. T. Laaksonen, O. Cheshnovsky, and R. E. Smalley, J. Chem. Phys. **88**, 5377 (1988).
[7]S. T. Lee, G. Apai, M. G. Mason, R. Benbow, and Z. Hurych, Phys. Rev. B **23**, 505 (1981).
[8]M. G. Mason, Phys. Rev. B **27**, 748 (1983).
[9]S. B. Dicenzo and G. K. Wertheim, Comments Solid State Phys. **11**, 203 (1985).
[10]M. E. Lin, R. P. Andres, and R. Reifenberger, Phys. Rev. Lett. **67**, 477 (1991).
[11]J. W. Gadzuk and E. W. Plummer, Rev. Mod. Phys. **43**, 487 (1973).
[12]A. Modinos, *Field, Thermionic and Secondary Electron Emission Spectroscopy* (Plenum, New York, 1984).
[13]R. H. Fowler and L. W. Nordheim, Proc. R. Soc. London Ser. A **119**, 173 (1928).
[14]J. W. Gadzuk, Phys. Rev. B **1**, 2110 (1970).
[15]C. B. Duke and M. E. Alferieff, J. Chem. Phys. **46**, 923 (1967).
[16]J. R. Oppenheimer, Phys. Rev. **31**, 66 (1928).
[17]J. M. Eisenberg and W. Greiner, *Nuclear Theory Vol. 1* (North-Holland, Amsterdam, 1970).
[18]T. Castro, Y. Z. Li, R. Reifenberger, E. Choi, S. B. Park, and R. P. Andres, J. Vac. Sci. Technol. A **7**, 2845 (1989).
[19]I. S. Gradshteyn and I. M. Ryzhik, *Tables of Integrals, Series, and Products* (Academic, New York, 1980).
[20]W. A. Harrison, Phys. Rev. **123**, 85 (1961).